Mechanical properties of alkali treated plant fibres and their potential as reinforcement materials II. Sisal fibres

L. Y. MWAIKAMBO*
Department of Engineering Materials, University of Dar es Salaam, P.O. Box 35131, Tanzania
E-mail: lymwaikambo@udsm.ac.tz

M. P. ANSELL
Department of Mechanical Engineering, University of Bath, Bath, BA2 7AY, United Kingdom

Published online: 3 March 2006

The tensile strength and Young's modulus of sisal fibre bundles were determined following alkalisation. The results were then analysed with respect to the diameter and internal structure such as cellulose content, crystallinity index and micro-fibril angle. The tensile strength and stiffness were found to vary with varying concentration of caustic soda, which also had a varying effect on the cell wall morphological structure such as the primary wall and secondary wall. The optimum tensile strength and Young's modulus were obtained at 0.16% NaOH by weight. The stiffness of the sisal fibre bundles obtained using the cellulose content also referred to as the micro-fibril content was compared with the stiffness determined using the crystallinity index. The stiffness obtained using the crystallinity index was found to be higher than that obtained using the cellulose content however, the difference was insignificant. Alkalisation was found to change the internal structure of sisal fibres that exhibited specific stiffness that was approximately the same as that of steel. These results indicates that the structure of sisal fibre can be chemically modified to attain properties that will make the fibre useful as a replacement for synthetic fibres where high stiffness requirement is not a pre-requisite and that it can be used as a reinforcement for the manufacture of composite materials.

1. Introduction

There is an increasing interest in research for in-depth understanding of the structure-property characteristics of plant fibres. This entails how this relationship can be tailored to meet requirements that would suit certain functionalities. Reinforcement for polymers is an area where research has concentrated in recent years. The bench mark for the required properties has been areas where synthetic fibres are dominating particularly in composite materials. However, optimum properties in synthetic fibre reinforced composites tested in tension can only be acquired for unidirectional lying of the fibres.

The unidirectional arrangement of plant fibres in composites is complicated by the existence of the inherent composite nature they possess [1] thus necessitating the need for research to study this unique structure. It has been demonstrated in literature that there exist a strong correlation between the structure and properties of plant fibres. For instance, the strength is said to be attributed to the rigidity and high molecular weight of cellulose chains, intermolecular and intramolecular hydrogen bonding and fibrillar and the crystalline structure of the fibres [2]. The strength and stiffness of fibres have also been shown to be dependent on the crystallinity index and micro-fibril angle.

McLaughlin and Tait [3] have showed that strain is more dependent on the micro-fibril angle and that it increases with increase in the micro-fibril angle. Fibres with higher cellulose content have also been found to be stronger than those with low cellulose content as long as their micro-fibril angle is small. Sisal fibre with a micro-fibril angle between 10–22 and cellulose content of over 70% [4, 5]

*Author to whom all correspondence should be addressed.
0022-2461
DOI: 10.1007/s10853-006-5075-4

exhibit inferior mechanical properties to hemp and flax fibres, which have micro-fibril angles of less than 7° and cellulose content of over 90% [6].

The above-mentioned characteristics make the fibres attractive materials for end uses such as reinforcements for polymeric materials. The mechanical properties reflect the orientation of the micro-fibrils, which are inclined at an angle to the cell axis.

1.1. Modelling the stiffness of the cellulose cell wall

There is a strong correlation between the micro-fibril angle (θ) and the Young's modulus of the fibres. Models indicate that fibre stiffness is influenced by the spiral angle of the crystalline fibrils as well as the concentration of non-crystalline materials [7, 8]. These structural parameters vary between the different types of natural fibre accounting for some of the variations in reported fibre properties. The effect on the mechanical properties of increased micro-fibril angle plays an important role when determining the mechanical properties of fibre-reinforced composites. It is necessary to measure the alignment of micro-fibrils applied to plant fibres to the direction of the force especially in determining tensile properties, bearing in mind that plant fibres exhibit significant mechanical anisotropy. A theoretical analysis of the way a fibre behaves when stretched may in practice represent the behaviour of fibre-reinforced composites when determining their mechanical properties. In this case a uniform strain theory has been used to obtain an estimate of the stiffness of the entire arrangement in both the fibre and the cell wall composite material. The theory uses an assembly of springs tied together so that they all receive the same displacement μ under a tensile load F as shown in Fig. 1. The theory is based on the work of Bodig and Jayne [9]. $\bar{\mu}$ and $\bar{F}$ is the mean displacement and load on the micro-fibrils respectively. K_1 and K_2 are the micro-fibril constants.

The overall stiffness of the system of the fibre in the fibre axis is given by Equation 1.

$$\bar{k} = \sum K_i \cos^2 \theta_i \tag{1}$$

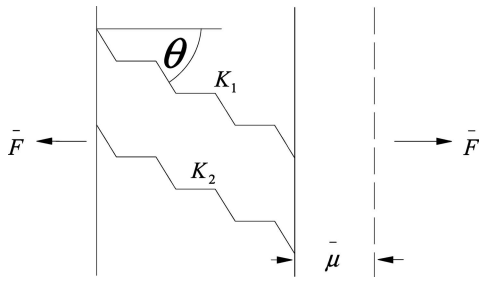

Figure 1 Arrangements of a uniform elastic deformation model in the plant fibre cell wall.

If $\bar{k}$ = overall stiffness of the fibre (E_f) and K_i is the stiffness of the micro-fibrils (E_s) then Equations 1 becomes 2.

$$E_f = E_S \cos^2 \theta \tag{2}$$

Equation 2 gives the longitudinal Young's modulus of plant fibres measured in tension. Efforts are being made to determine the transverse Young's modulus of plant fibres but this is not covered here. However, Cichocki and Thomason [10] used an environmental scanning electron microscopy (ESEM) equipped with a load frame to measure the Young's modulus of a carefully sectioned array of wood cells in the transverse direction. Their measurement indicated that the transverse Young's modulus varied with the type of wood used and was less than the longitudinal Young's modulus [9].

1.2. Modelling of the cell wall as a composite material

Since both the crystalline and non-crystalline region will deform, the applied load is shared between these two components just as is the case with the composites. The determination of stiffness properties of plant fibres can be predicted by using the rule of mixtures (ROM). For instance, Equation 3 is used to estimate the stiffness or modulus of elasticity of the plant fibre cell wall [11, 12] along the fibre axis. The effective modulus of the fibre (E_f) is given in terms of the amounts of participating components present in the fibre. The ROM takes into consideration the masses of the crystalline and non-crystalline cellulose to determine the stiffness of the composites (Equation 3).

$$E_f = V_c E_c \cos^2 \theta + V_{nc} E_{nc} \tag{3}$$

where, E_c and E_{nc} are the moduli of crystalline and non-crystalline regions and V_c and V_{nc} are the volume fractions of crystalline and non-crystalline regions. Kulkarni *et al.* [11] reported elastic moduli of the crystalline and non-crystalline regions for vegetable fibres as 45 GPa and 3 GPa respectively. When banana fibre was tested at a micro-fibril angle of 12° and 11°, with a fibre diameter of 100 μm with volume fractions of 0.65 and 0.35 for crystalline and non-crystalline components respectively, the modulus values obtained using Equation 3 compared well with the practical modulus values obtained by Kulkarni *et al.* [11] when determining the mechanical properties of banana fibres *Musa sepientum*. Mukherjee *et al.* [12] performed similar work on sisal fibre tested at different test gauge lengths and speeds and the results obtained were comparable to the theoretical predictions.

1.3. Fibre modifications

The main requirement for reinforcement is to use stiff fibres and a well-bonded fibre-matrix interface with the ultimate aim of reaching the stiffness of conventional synthetic reinforcement such as carbon and glass fibres. In plant fibres these requirements are partially attained by alkali treatment.

Sisal fibres possess surface impurities such as wax and natural oils and sometimes processing oils can also be deposited at the surface. Bleaching and/or scouring using solvents can remove these surface impurities. Several fibre modification processes in textile manufacturing require the removal of these surface impurities to improve lustre and dye uptake. In composite manufacture removal of surface waxy materials improves mechanical interlocking and reactivity with the resins thus developing strong interfacial adhesion. Cellulose forms the main structural constituent of plant fibres and contributes immensely to the mechanical properties of plant fibres. Other components such as lignin and hemicelluloses play an important part in the characteristic properties of the fibres. Toughness, that is the tendency of plant fibres to absorb energy in impact, is decreased with a decreasing amount of lignin and/or hemicelluloses while at the same time the strength and stiffness of the fibre is increased up to a limit. The development of fibre-reinforced composites favours the use of stiff fibres for reinforcement of polymeric materials.

Removing lignin and hemicelluloses thus leaving stiffer cellulose can produce stiff plant fibres. The removal of hemicelluloses leaves a less dense and less rigid interfibrillar region allowing the fibrils to re-arrange along the fibre major axis [12]. Stretching the fibre results in better load sharing by the fibrils hence higher stress development in the fibre. On the other hand, softening of the interfibrillar matrix adversely affects the stress transfer between the fibril and thereby the overall stress development in the fibre under tensile deformation. Removing the lignin makes the middle lamella joining the ultimate cells become more plastic and homogeneous due to the gradual elimination of micro-voids whereas the ultimate cells themselves are only slightly affected. The rearrangement of the fibrils along the fibre axis and the resulting homogeneity of the ultimates lead to a packing order with increased crystallinity index for the plant fibres. Physical methods such as heating/drying can be applied to plant fibres to remove hemicelluloses, which are sensitive to high temperatures. The steam explosion technique is another method commonly used to produce clean fibres. Several chemical methods have been applied to modify plant fibres and these are discussed in the following sections together with physical methods.

In this work sisal fibre bundles that have been alkalised have been tested in tension and the results compared with conventional synthetic fibre reinforcements to assess the potential of sisal fibre as an alternative to synthetic fibres. Also, the theoretical stiffness of plant fibres has been predicted and results compared with experimental values.

2. Experimental methods

Sisal fibre used in this work was kindly supplied by the TBC (1998) Limited Tanzania. No specifications were available regarding the physical characteristics of the supplied fibres such as staple length, density, diameter and processing conditions. Sodium hydroxide pellets of 98% strength and glacial acetic acid were supplied as general laboratory reagents. Fibre were weighed and soaked in concentrations of 0.03, 0.08, 0.16, 0.24 and 0.32% sodium hydroxide for 48 h. They were washed in distilled water to which drops of glacial acetic acid were added to neutralise excess sodium hydroxide. They were then dried and placed in conditioning chambers for at least 48 h.

The diameter was determination using the scanning electron microscopy (SEM) and image analysis techniques the surface morphology analysis of un-fractured and tensile fractured fibres was performed using the SEM [6]. The cellulose content of plant fibres was calculated using a combination of the bulk, absolute and cellulose densities using Equation 4. A full description of the way densities were determined is provided in our earlier publications [13] and will not be repeated in this paper.

$$Z = \left[2\left(\frac{\rho_b}{\rho_a} + \frac{\rho_a}{\rho_{\text{cell}}}\right) - \frac{\rho_b}{\rho_{\text{cell}}} - 2\right] 100 \qquad (4)$$

where ρ_a, ρ_b, ρ_{cell} and Z are the absolute, bulk (apparent), cellulose densities, and cellulose content respectively.

The Instron tensile tester was used to determine the tensile properties. Thirty two specimens were tested in each case and results analysed.

3. Results and discussion

3.1. Surface topography and transverse sections

Figs 2a and b shows longitudinal and cross sectional views respectively of untreated sisal fibre bundles. Node-like cell materials indicated by arrows are seen holding together adjacent ultimate fibres. The cross sectional view (Fig. 2b) shows small and large lumens each representing a single ultimate fibre of hexagonal shape examples of which are shown by arrows. Following 0.24% NaOH treatment (Fig. 3a) the loose materials at the node-like cell wall features connecting the fibres is reduced in size implying that it has been dissolved by caustic soda. It is believed that these loose materials are part of the primary cell wall, which is highly soluble in caustic soda. The cross sectional view of the 0.24% NaOH treated sisal fibre bundles (Fig. 3b) shows ultimate fibres that are beginning to separate from one another (see arrows) It is the ultimates with wider lumen where the separation is

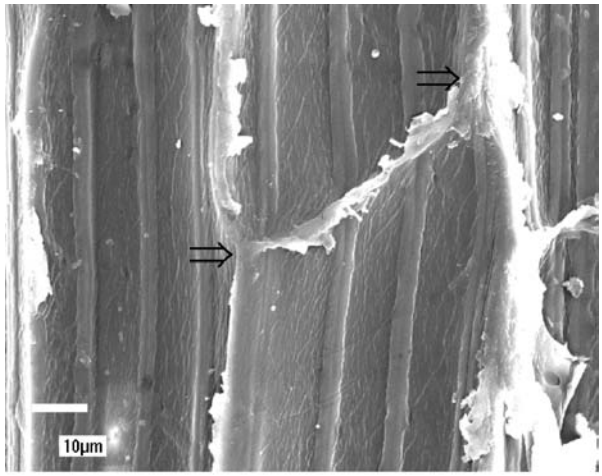

(a)

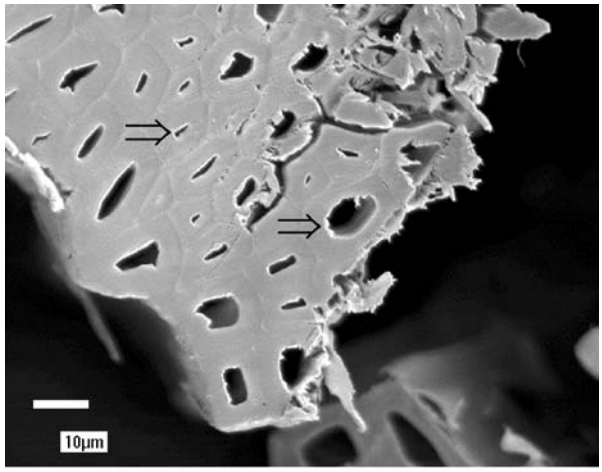

(b)

Figure 2 (a) Longitudinal and (b) cross sectional view of untreated sisal fibre.

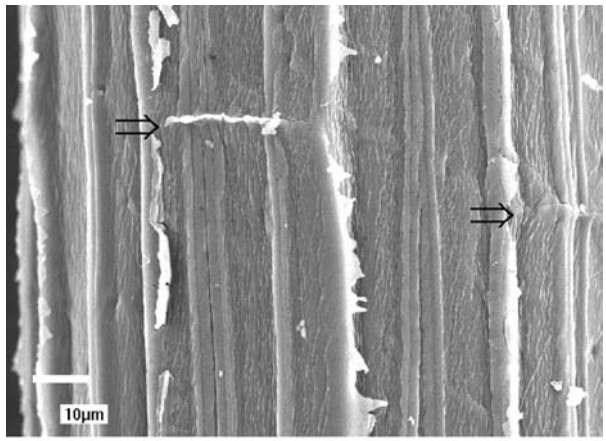

(a)

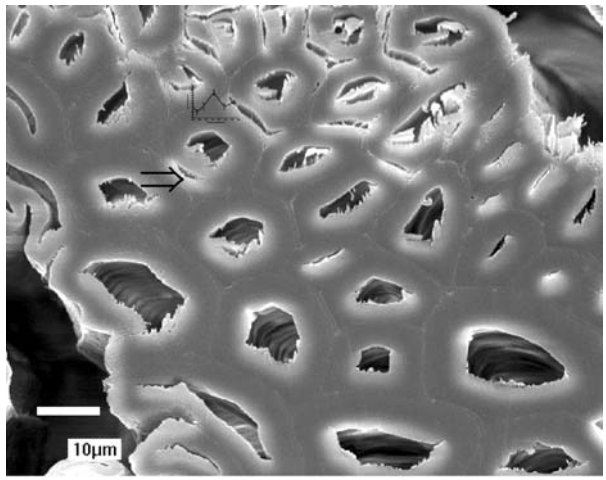

(b)

Figure 3 (a) Longitudinal and (b) cross sectional view of 0.24% NaOH treated sisal fibre.

visible than ultimates with narrow or closed lumen. It is possible that outward swelling is due to the depolymerisation of the densely packed crystalline region in the S_2 layer, which constitutes the main part of the cell wall.

Figs 4a and b show longitudinal and cross sectional views of 16% NaOH sisal fibres bundles. The longitudinal view shows open spiral vessels winding along the fibre length and is considered to be pathways for fluids in the sisal leaf. Clean individual ultimate fibres are visible. The absence of node-like cell wall materials indicates that the primary wall has been completely removed by caustic soda treatment. Binding materials such as lignin have been removed and hemicelluloses have been dissolved. The cross sectional view of the 16% NaOH treated sisal fibre (Fig. 4b) shows ultimate fibres with clear boundaries of adjacent cells some of which are beginning to separate (see arrows). The cells this time exhibit inward swelling and that in some of them the hexagonal shape has started to disappear. This implies that caustic soda has attacked and started to depolymerise the crystalline region in the S_3 layer. The differences in swelling within the cell wall will have significant impact on the mechanical properties of sisal fibres.

3.2. Effect of the fibre diameter

Following alkalisation the dependence of mechanical properties on the diameter of sisal fibre bundles is illustrated in Fig. 5. The diameters and tensile properties of untreated and alkali treated sisal fibre bundles were determined as described in Section 2.

The high strength and modulus (Figs 5 and 6 respectively) of small diameter fibre bundles is understandable since, in the limit, a single unbroken chain of cellulose molecules must be approaching the theoretical tensile strength of bonds between atoms. It is observed that the separation of ultimate fibres is optimised at around 0.16% NaOH (Figs 5 and 6). The increase in diameter and the drop in tensile strength (Fig. 5) and Young's modulus (Fig. 6) between 0% NaOH and 0.03% NaOH are due to the degradation of the primary wall. This level of caustic soda concentration (0.03% NaOH) will have a bleaching effect and will remove all the impurities on the surface

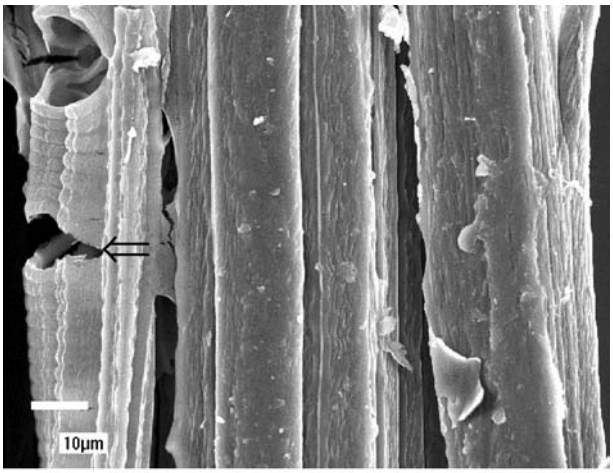

(a)

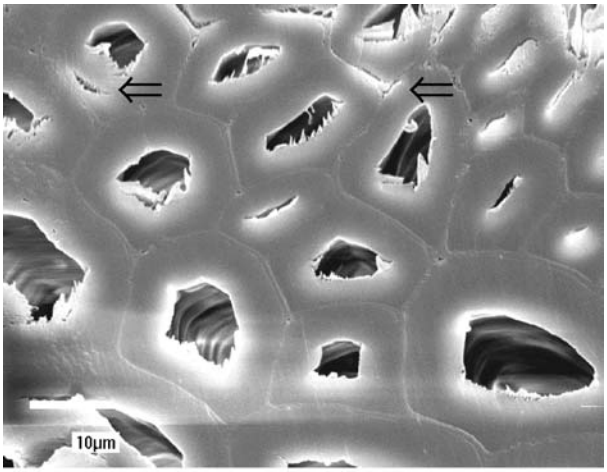

(b)

Figure 4 (a) Longitudinal and (b) cross sectional view of 16% NaOH treated sisal fibre.

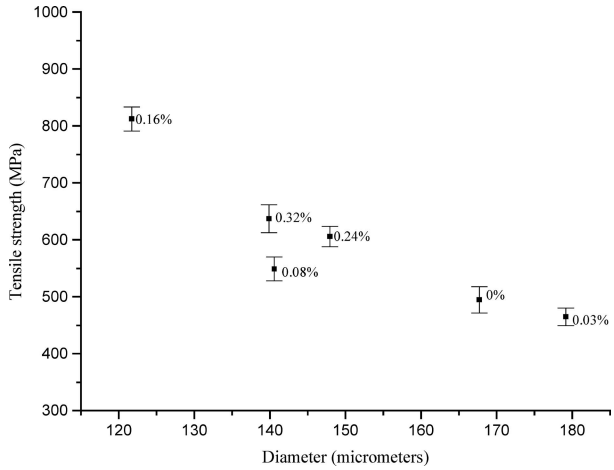

Figure 5 The strength of sisal fibre bundles with respect to fibre bundle diameter.

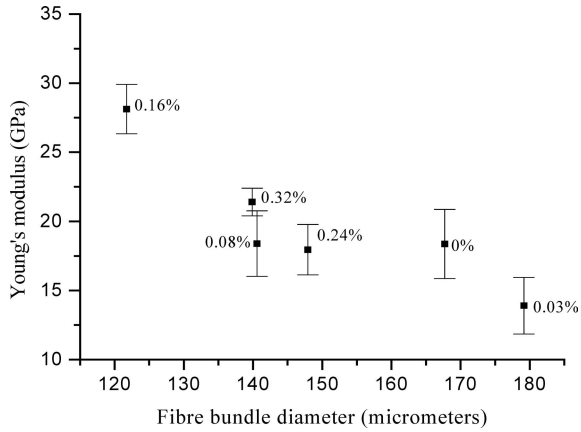

Figure 6 The modulus of sisal fibre bundles with respect to fibre bundle diameter.

of the fibre. Beyond 0.03% NaOH pectin is degraded and removed together from the cell wall causing separation of the ultimate fibres thus decreasing the diameter of the bundle. The closely packed crystalline region in the secondary wall (mainly S_1 and S_2) starts to open and exhibit improvement in the packing order of the crystalline region. Most of the lignin is removed between 0.03% NaOH and 0.16% NaOH without causing significant swelling of individual ultimate fibres.

The increase in the tensile strength and Young's modulus between 0.03% NaOH and 0.16% NaOH is firstly due to the removal of lignin, secondly and most important it is due to the decreased in diameter of the bundle. The increase in diameter of sisal fibre bundles between 0.16% NaOH and 0.24% NaOH is due to the swelling of the cell wall that occur mainly in the S_2 layer accompanied by degradation of the crystallites and increase in the amorphous regions. These changes in the S_2 layer cause decrease in the tensile strength and Young's modulus of the sisal fibre bundles (Figs 5 and 6). Increase in the tensile strength between 0.24% NaOH and 0.32% NaOH is due to improved packing of the crystalline region in the S_3 layer of the cell wall together with densification in the S_2 layer.

The degradation of the cell wall, appear progresses inwardly, from the primary wall towards the secondary wall, as shown in Scheme 1 below.

$$\text{Primary wall} \rightarrow S_1 \rightarrow S_2 \rightarrow S_3$$

Scheme 1 Hypothetical pathway model of progressive swelling of the cell wall following alkalisation.

The rate of absorption of NaOH solution and the compactness of the crystalline cellulose in the four layers is shown in Scheme 1. The equilibrium at which the absorption will occur will be different from one layer to another until an overall equilibrium is attained. The mechanical properties of alkalised fibres will depend on the concentration of NaOH and on the sorption time.

3.3. The effect of cellulose content

Figs 7 and 8 shows the effect of cellulose content on the tensile strength and Young's modulus of alkalised sisal fibre bundles. Following 0.08% NaOH treatment sisal fi-

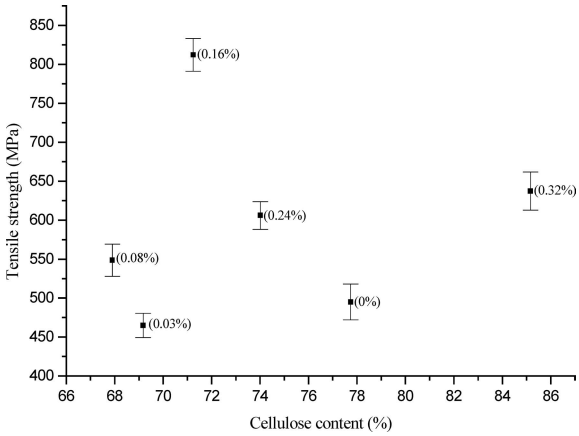

Figure 7 The effect of cellulose content on the tensile strength of sisal fibre bundles.

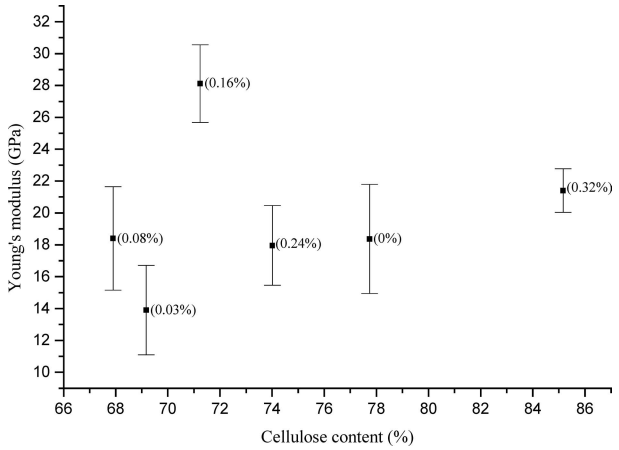

Figure 8 The effect of cellulose content on the Young's modulus of sisal fibre bundles.

bre bundles exhibits a decrease in cellulose content of about 13% that in turn causes increase in tensile strength of about 11%. The decrease in cellulose content and increase in tensile strength between untreated and 0.08% NaOH treatment is believed to be due to the degradation of the primary wall and improved packing order of crystallites mainly in the S_1 layer. However, increase in the cellulose content between 0.08% NaOH and 0.16% NaOH is due to the decrease in the non-cellulose materials present in the primary wall and the S_1 layer. At this stage the packing order of crystalline region in the S_2 layer is increased resulting in approximately 64% increase in the tensile strength (Fig. 7) and 53% increase in the Young's modulus (Fig. 8). Mukherjee *et al.* [12] and Murkhejee [14] reported the correlation of the increase in the amorphous cellulose following caustic soda treatment at the expense of a decrease in the crystalline cellulose. Also following alkalisation, release in the strain occurs in the crystallites, which results in improved packing order along the longitudinal direction of the fibre [8] with the subsequent increase in mechanical properties.

3.4. The effect of crystallinity index

Following alkalisation of the sisal fibre bundles both the tensile strength (Fig. 9) and Young's modulus (Fig. 10) show the same pattern of changes in the crystallinity index with respect to changes in the concentration of caustic soda, and the effect these changes has on the tensile strength and Youmg's modulus of the fibres. The crystallinity index is calculated using Equation 5 [15].

$$I_C = \frac{\left(I_{(002)} - I_{(am)}\right)}{I_{(002)}} \times 100 \qquad (5)$$

where I_C, $I_{(002)}$ and $I_{(am)}$ are the crystallinity index, reflection at 002 due to crystalline cellulose and the reflection due to amorphous regions respectively. The increase in the crystallinity index between untreated and 0.03% NaOH treated sisal fibre is caused by a decrease in pseudo amorphous material. The 0.03% NaOH concentration is not strong enough to cause significant swelling of the cell wall but sufficient to remove non-cellulose (impurities) on the surface of the fibre including the primary wall. The

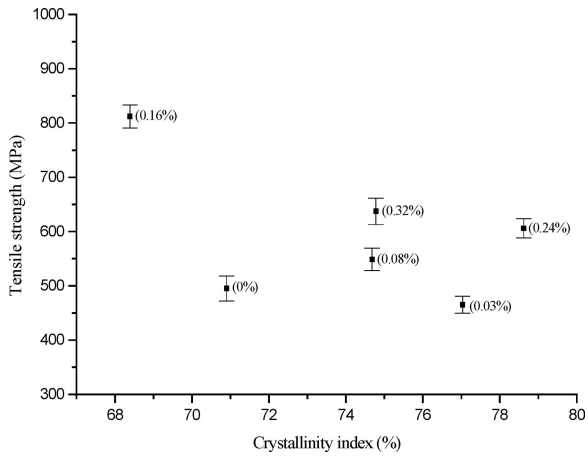

Figure 9 The dependence of tensile strength of sisal fibre bundles on the crystallinity index.

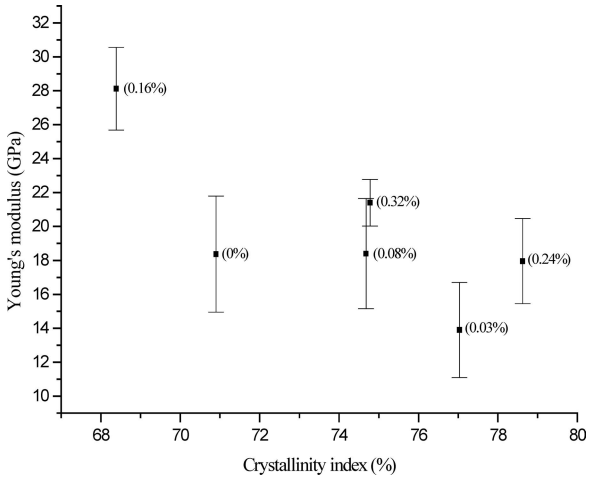

Figure 10 The dependence of Young's modulus of sisal fibre bundles on the crystallinity index.

X-ray will record the pseudo and genuine amorphous materials as amorphous regions. However, because part of the primary wall is degraded, it will result in a decrease in the tensile strength (Fig. 9) and Young's modulus (Fig. 10), partly because the crystalline cellulose in the primary wall will have not formed ordered crystalline regions.

Increasing the concentration of caustic soda beyond 0.03% and up to 0.16% degrades crystalline regions decreasing the intensity of the 002 reflection whilst increasing amorphous regions [15]. These changes in the crystalline regions with respect to changes in caustic soda concentration cause improvement in the crystalline packing order. It is worth pointing out that it is the S_1 and S_2 cell wall layers that are mostly affected between 0.03% NaOH and 0.16% NaOH concentrations. The packing order of the crystalline regions in S_2 layer is optimised at 0.16% NaOH beyond which the crystalline cellulose degrades without significant improvement in the packing order causing a decrease in the tensile strength and Young's modulus up to 0.24% NaOH. Increasing the concentration of caustic soda to 0.32% results in slight increase of the amorphous regions in the S_2 layer and improvement in the packing order in the S_3 followed by consolidation of the crystalline regions which in turn causes increase in the tensile strength (Fig. 9) and Young's modulus (Fig. 10). It has been reported that following alkalisation sisal fibre exhibit different degradation profile across the cell wall [16] and that the primary wall including part of the S_1 layer are plasticised. The inner layer which constitutes the S_2 and S_3 layer and is not plasticized. This different reaction of the sisal fibre cell wall to caustic soda treatment have been exploited to develop self-reinforced sisal fibre composites where the outer plasticized layer functions as the binding materials to the not plasticised inner layer which acts as the reinforcement [16].

3.5. The effect of the micro-fibril angle

The initial postulated stiffness model of the micro-fibril inclined at an angle θ to the fibre major axis has been presented in Equation 2. The general equation for the stiffness of plant fibres is has been fully explained in a previous publication [6]. For the purpose of determining the micro-fibril angle of sisal fibre bundles Equation 3 is modified to obtain Equation 6. The micro fibrils are arranged in fabric-like layers known as lamellae, which exhibit alternately either a Z or S winding direction [7]. Using Equation 6 an estimate of the micro-fibril angle θ was determined:

$$\theta = \mathrm{Cos}^{-1}\sqrt{\left(\frac{E_f - (1 - V_S)E_L}{V_S E_S}\right)} \tag{6}$$

where, V_S, E_S and E_L are volume fraction, elastic modulus of micro-fibrils and elastic modulus of non-crystalline regions (mainly lignin).

Only the micro-fibril angle of untreated fibres was determined (19.7°) and this is shown in Table I.

In order to evaluate the elastic moduli of the micro-fibrils it was assumed that following alkalisation (a) the micro-fibril angle and (b) the stiffness of the non-cellulose material remain the same. It is worth noting that caustic soda does not degrade lignin hence validating the second assumption. While the first assumption may not strictly be valid, combined with the second assumption acceptable results for the stiffness of the fibre and cellulose content in untreated and alkali treated sisal fibre bundles are obtained and are shown in Table I.

Table I indicates that the stiffness of the fibre (E_f) is approximately 31% lower than the stiffness of the micro-fibrils (cellulose). The decrease in the stiffness of the fibre from that of the micro-fibrils is the result of resolving the forces with respect to the angle of inclination to the longitudinal axis of the fibre and the presence of the non-cellulose materials mainly lignin. Table I also shows the micro-fibril angle (19.7°) that is within and close to the higher values reported in literature [9, 12]. The variation in the micro-fibril angle between experimental and literature value is also attributed to differences in the environmental testing conditions.

Using the stiffness model of plant fibres (Equation 3) and the physical and structural properties of sisal fibre bundles [12] including the literature values of the stiffness of lignin, 3.0 and 3.4 GPa, reported by Kulkarni *et al.* [11] and McLaughlin and Tait [3] respectively. Estimates of the elastic moduli (E_S) of the micro-fibrils (E_S is also referred to a E_Z) were determined as a function of firstly cellulose content (Z) and secondly crystallinity index (Z) and are shown in Table II. The stiffness of the micro-fibrils (E_S) obtained using the cellulose content and the stiffness of the micro-fibrils obtained using the crystallinity index were obtained using Equations 7 and 8 respectively.

$$E_S = E_Z\left[\frac{E_f - (1 - V_Z)E_L}{V_Z \mathrm{Cos}^2\theta}\right] \tag{7}$$

$$E_I = \left[\frac{E_f - (1 - V_I)E_L}{V_I \mathrm{Cos}^2\theta}\right] \tag{8}$$

where, V_Z, V_I are volume fraction of cellulose content and crystallinity index respectively.

Equations 7 and 8 were developed and used to determine the stiffness of the micro-fibrils with respect to the

TABLE I. Estimate of the micro-fibril angles of untreated sisal fibre bundles as a function of cellulose content (Z)/micro-fibril content

Fibre type	Sisal
V_Z	0.7774
E_Z (GPa)	24.06
E_f(GPa)	18.37
θ (°)	19.7

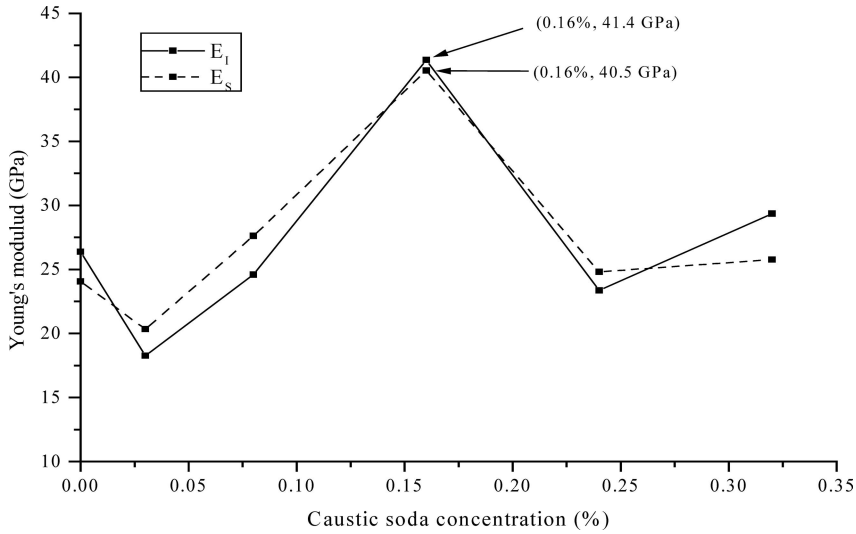

Figure 11 The stiffness of micro-fibrils of sisal fibre bundles with respect to crystallinity index and cellulose content.

cellulose content and crystallinity index of the sisal fibre. Fig. 11 was used to illustrate the difference in the stiffness with respect to the cellulose content (micro-fibril content) and crystallinity index. It was observed that untreated sisal fibre exhibits higher stiffness using the crystallinity index than using the cellulose content. However, following alkalisation, the stiffness obtained using the cellulose content (micro-fibrils) become higher than the stiffness calculated using the crystallinity index, implying that as the concentration of the caustic soda is increased the crystallites becomes more ordered with a decrease in the micro-fibril angle. Several researchers have reported that fibres with lower micro-fibril angle exhibits higher stiffness than fibres with higher micro-fibril angle [7, 11–13].

The moduli E_I and E_S reaches a maximum at 0.16% NaOH with insignificant variation when the stiffness values are approximated to whole number integer. At higher concentration of caustic soda the stiffness obtained using the crystallinity index is higher than that obtained using the cellulose content due to the consolidation of the crystallites as the non-cellulose materials are removed.

The micro-fibril angle used in this work was that calculated using untreated fibres. However, it will change with changes in the concentration of caustic soda used to treat the sisal fibres.

Table II shows that the elastic modulus (E_I) values of the crystalline material determined using the crystallinity index (Equation 8) are higher than values of elastic modulus (E_S) determined using the micro-fibril or cellulose content (volume fraction of cellulose) (Equation 7). This indicates that crystallinity index is a better measure of the plant fibre's stiffness than cellulose content.

TABLE II. The stiffness of the micro-fibrils of sisal fibre bundles calculated as a function of crystallinity index (I) and cellulose content (Z)

Treatment (% NaOH)	0	0.03	0.08	0.16	0.24	0.32
E_I (GPa)	26.38	18.26	24.60	41.36	23.36	29.35
E_Z (GPa)	24.06	20.34	27.62	40.53	24.81	25.77

The results also show that the lower stiffness values obtained using the cellulose content is a result of the presence of tiny air pockets [17] and the lignin content and hemicelluloses which reduce stiffness. The stiffness values obtained in Table II are close to stiffness values obtained by McLaughlin and Tait [3] and Kulkarni *et al.* [11] using bowstring hemp (*Sansevieria metallica* Géróme and Labroy) and banana (*Musa sepintum*) fibres respectively.

3.6. The effect of caustic soda on tensile properties

The effect of alkali treatment on the mechanical properties of sisal fibre bundles was studied. The nature and texture of the fibre bundles are not the same in their natural or alkalised states. For instance, the average diameter and density of the untreated and alkali treated sisal fibre bundles have previously been found not to be the same [18]. These factors will affect the mechanical properties of the fibres, which exhibit large variations in mechanical properties.

Figs 12 and 13 shows the tensile strength and Young's modulus of untreated and alkalised sisal fibre bundles. A decrease in tensile strength and Young's modulus with increase in the concentration of caustic soda up to 0.03% NaOH is observed. Beyond this concentration the strength and stiffness increases sharply and reaches a maximum at 0.16% NaOH and then falls. The fall in tensile strength and Young's modulus between 0.16% NaOH and 0.24% NaOH is due to the degradation of the crystalline cellulose in the S_2 layer. The tensile strength and Young's modulus increase slightly between 0.24% and 0.32% NaOH due to densification of the crystalline cellulose.

The tensile strength versus Young's modulus of sisal fibre bundles has been plotted and is shown in Fig. 14. A

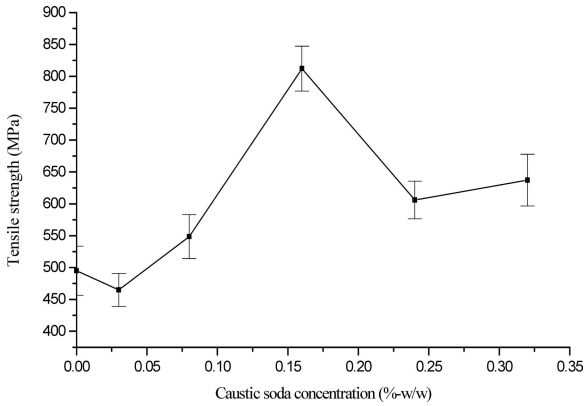

Figure 12 Tensile strength of untreated and alkalised sisal fibre bundles with respect to caustic soda concentration.

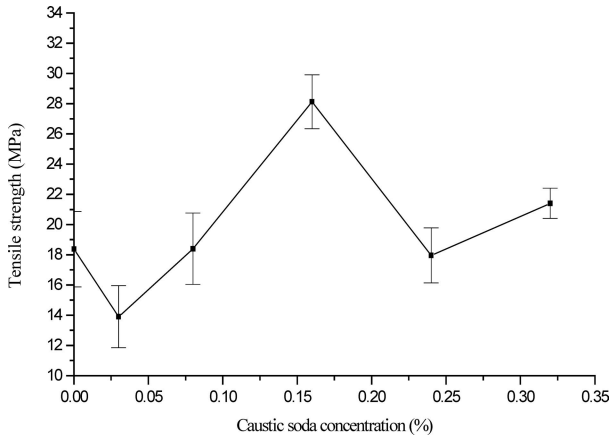

Figure 13 Young's modulus of untreated and alkalised sisal fibre bundles with respect to caustic soda concentration.

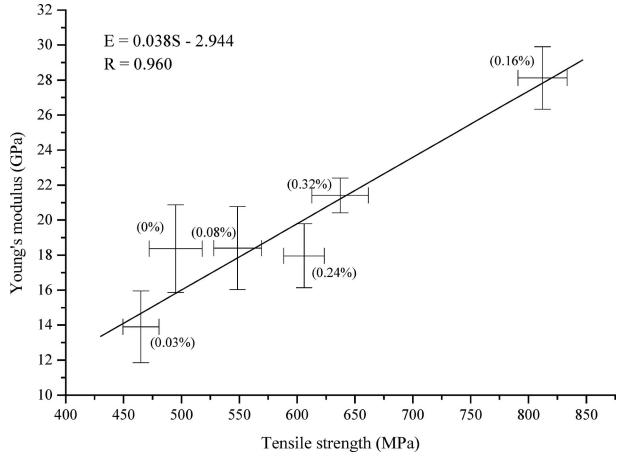

Figure 14 Young's modulus vs Tensile strength of untreated and alkalised sisal fibre bundles.

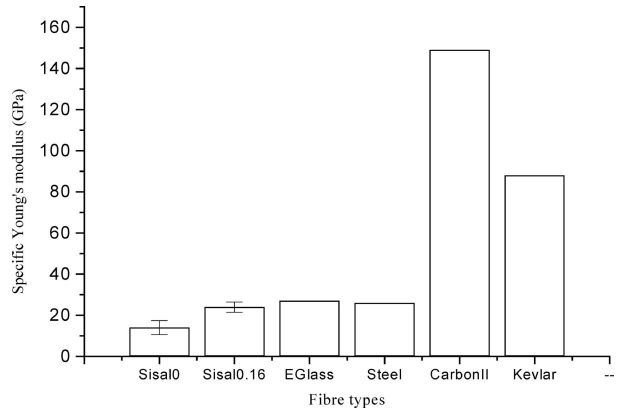

Figure 15 Specific Young's modulus versus untreated and 0.16% NaOH treated sisal fibre bundles and some man-made fibres.

regression line through the data points is shown and an equation (Fig. 14 inset) has been provided where E and S are the Young's modulus and tensile strength respectively. The linear relationship of the plots illustrates the theoretical model available in literature [18, 19]. The variation of the scatter of the points (Fig. 14) is not significant indicating good test control and that the fibre's weak places, which would result in stress concentrations, are evenly distributed and minimal.

3.7. Comparison between sisal, steel and synthetic fibres

The specific modulus is plotted for untreated and alkali treated sisal fibre bundles and high-performance fibres (Fig. 15) namely Kevlar 29, Carbon Type II, E-Glass and steel fibres. The specific modulus of untreated sisal fibre bundles is approximately 86% and 93% less stiffer than that of steel and E-glass respectively. Sisal fibre bundles treated at 0.16% caustic soda concentrations exhibit about 8% and 13% less specific modulus than steel and E-glass respectively

Following alkalisation the specific modulus of sisal fibre bundles increases significantly. This implies that for sisal fibre to compete with steel and E-glass fibres its internal structure need to be modified using caustic soda

However, the good performance of the synthetic fibres is mainly due to their well engineered structure such as linearity and very small diameter compared to plant fibre bundles, which possess a hollow non-linear molecular structure coupled with the presence of natural and processing defects along the fibre length. These results show that plant fibres can provide useful replacements for steel and synthetic fibres where specific stiffness is not a critical requirement.

3.8. Fracture surface topography of the fibre bundles

Sisal fibres have been found to consist of bundles of single ultimate cells as indicated in the SEM micrographs Figs 2–4 and also examined in this section. The fibres contain cell wall layers with the lumen space (indicated by arrows) at the centre. The fracture mechanism of plant fibres bundles has been well documented by McLaughlin and Tait [3], Kulkarni *et al.* [11] and Morton and Hearle [7]. Some authors have reported the fracture mechanism of plant

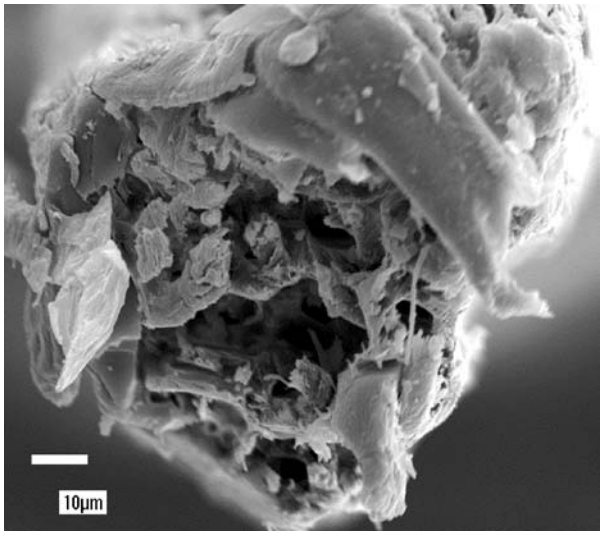

Figure 16 SEM micrograph of untreated sisal fibre bundle fractured in tension.

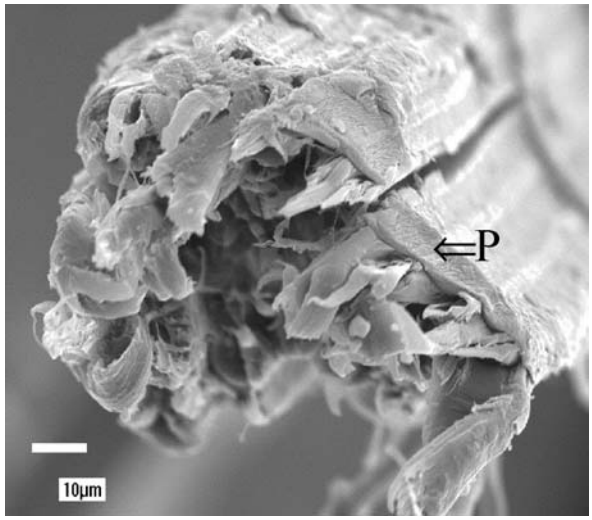

Figure 18 SEM micrograph of 0.08% NaOH treated sisal fibre bundle fractured in tension.

fibres when used as reinforcement for polymeric resins [20, 21]. In all these studies plant fibres show a fibrillar splitting and buckling fracture characteristics. Dinwoodie [22] and Davies and Bruce [23] carried out a study on micro-compressions in wood and flax fibres respectively and found that damaged fibres had lower tensile strengths and moduli. In this research the inherent (nodes) and processing defects in sisal fibre bundles are seen as the major sites for failure initiation in tensile loading. Figs 16–18 shows SEM micrographs of sisal fibre bundles fractured in tension.

Fig. 16 shows a brittle fracture of untreated sisal fibre bundle and cell wall delamination. Fibre pull-out is observed in the outer part of the bundle, which indicates lack of sufficient binding material (mostly lignin). The fracture failure at the centre of the bundle exhibit less fibre pull-out indicating the presence of sufficient binding material. Fractured fibre bundles also exhibit insignificant fibril splitting and more ultimate fibre buckling.

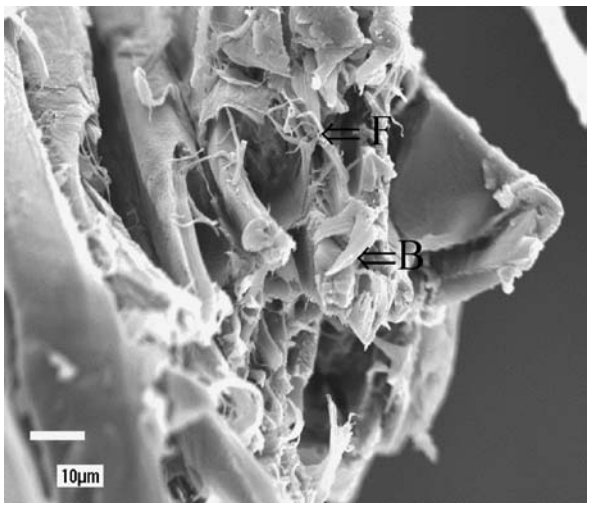

Figure 17 SEM micrograph of o.03% NaOH treated sisal fibre bundle fractured in tension.

Furthermore, the failure of the sisal fibre bundle is not at the same stress level indicating the presence of cell wall defects along the fibre, which then develops stress intensities leading to failure.

Fig. 17 shows brittle fracture of 0.03% NaOH treated sisal fibre bundle. The fracture mechanism is similar to that exhibited by the untreated sisal fibre bundle (Fig. 16), however, in this case separation of the ultimate fibres occurs in the outer part of the bundle. This indicates the removal of surface impurities and degradation of binding material in the outer part of the bundle. Fibre splitting is in the form of layers, which implies that the binding material between the layers has been degraded following alkalisation. The amount of fibres buckling (Fig. 17 B-arrow) due to the fracture is approximately the same as the amount of fibril buckling (Fig. 17 F-arrow).

Fig. 18 shows brittle fracture of 0.08% NaOH treated sisal fibre bundle. The fibre bundles consists outer layer covering the ultimate fibres. The outer layer exhibits clean surface with shallow ridges and troughs which are signs of ultimate cell morphological configuration. The outer layer is believed to be the result of a plasticized primary wall (Fig. 18 P-arrow), which can be used as binder material for the inner (core) layer to produce a self-reinforced sisal fibre composite [16].

Pull-out of the ultimate fibres occurs around the outer part of the bundles indicating that the binder material has been degraded following alkalisation. Ultimate fibres around the outer part of the bundle also exhibit buckling following fracture and insignificant splitting of the fibrils is observed. The minimal splitting of the fibres into fibrils is an indication of bulking of the cell wall and that the strain in the micro-fibrils has been relaxed.

Fig. 19 shows a fracture surface of 0.16% NaOH treated sisal fibre bundle. Fibre pull-out and buckling are ob-

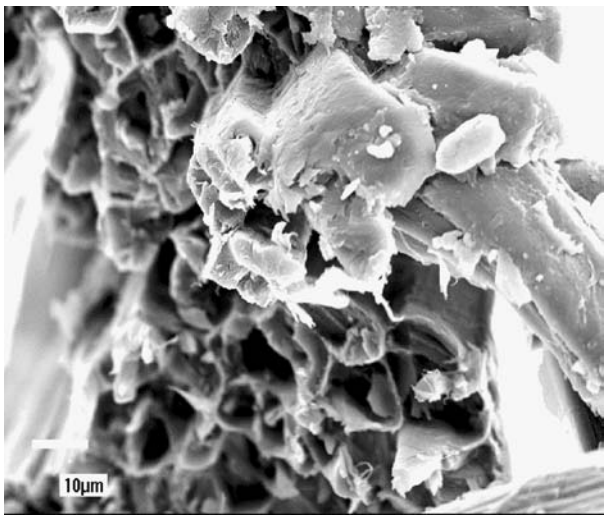

Figure 19 SEM micrograph of 0.16% NaOH treated sisal fibre bundle fractured in tension.

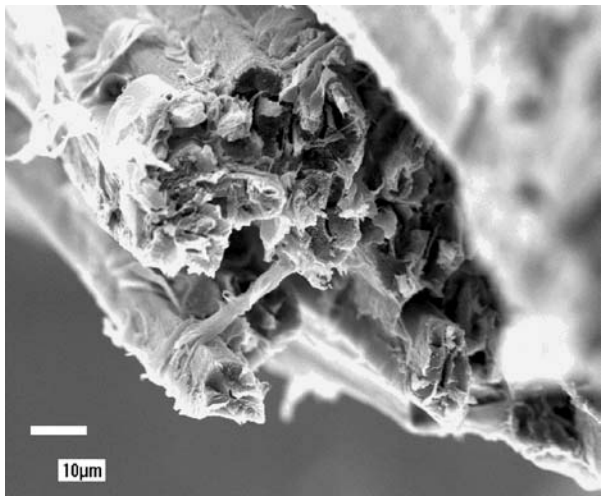

Figure 21 SEM micrograph of 0.32% NaOH treated sisal fibre bundle treated in tension.

served but to a lesser extent compared to fibres that have been treated using 0.08% NaOH. There a is noticeable absence of splitting of the single cells into fibrils and individual ultimate fibres at the centre of the bundle have fractured almost at the some level. This indicated that 0.16% NaOH has degraded the binding material, penetrated the cell wall and improved the packing order of the crystalline region. This re-organisation of the crystalline region will have significant increase in the tensile strength and Young's modulus of the sisal fibres.

Fig. 20 shows a 0.24% NaOH treated sisal fibre bundle fractured in tension. The ultimate fibres show significant swelling of the cell wall and have fractured at the same level. Minimal fibril splitting and buckling is observed indicating the relaxation of the strain in the micro-fibrils. Also the uncoiling of the spiral structure, indicated by an arrow (Fig. 20), is exhibited. The significant swelling of the cell wall and the uncoiling of the spiral structures

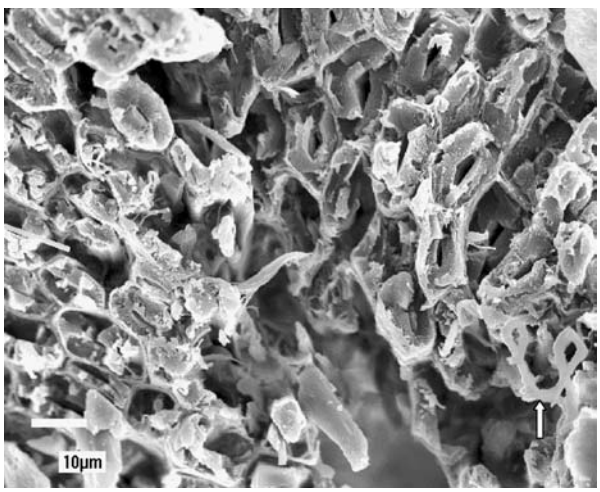

Figure 20 SEM micrograph of 0.24% NaOH treated sisal fibre bundle fractured in tension.

will impart a decrease in the tensile strength and Young's modulus of the sisal fibre bundle.

Fig. 21 shows a 0.32% NaOH treated sisal fibre bundle fractured in tension. The layer that was exhibited in Fig. 18 which was due to the plasticisation of the primary wall following 0.08% NaOH treatment is not observed. The absence of the plasticised material in Fig. 21 is an indication that caustic soda concentrations higher than 0.08% are not suitable for producing a plasticised outer layer binding material on sisal fibres.

Alkalised sisal fibre bundles at different caustic soda concentrations show different failure profiles and the fracture in these cases occurs at the same stress level, which is an indication together with reasons provided in previous sections that most of the weak points have been eliminated and/or uniform distribution of crystallites is attained. This is expected because alkalisation in plant fibres swells the fibre cell wall allowing the rearrangement of the crystallites into a well-ordered state thus reducing the number of weak places. By reducing the weak places the stress is then evenly distributed along the fibre length. The buckling and unravelling of ultimate fibres seen in sisal fibre bundles treated using low caustic soda concentration, seen in Figs 17 and 18 are an indication of the uncoiling of the micro-fibrils and the presence of the strain in the fibrils [6, 11].

4. Conclusions

The internal structure of sisal fibre can be modified using caustic soda up to a limit in order to improve its performance. The SEM micrographs of untreated and alkalised sisal fibres show rough and void regions between individual fibre cells. The study has shown that the tensile strength and Young's modulus of sisal fibre bundles depends on the physical characteristics of its internal structure such as the cellulose content, crystallinity index and micro-fibril angle. The introduction of a rough surface will

facilitate mechanical interlocking with the resin-matrices resulting in enhanced interface while improved packing order of the crystalline regions following alkalisation increases the tensile strength and stiffness of the sisal fibre making it suitable as reinforcement for the manufacture of composites.

Acknowledgments

The authors are grateful to the Norwegian funding agency, NORAD, for their financial support during the time of conducting the research

References

1. R. E. MARK, In "Theory and design of wood and fibre composite materials", edited by B. A. Jayne, (Syracuse University Press, New York 1972) p. 49.
2. T. NGUYEN, E. ZAVARIN and E. M. BARRALL, J. MACROM, *Sci. Rev. Macrom. Chem.* **C20** (1981) 1.
3. E. C. MCLAUGHLIN and R. H. TAIT, *J. Mater. Sci.* **15** (1980) 89.
4. D. R. PERRY, "Identification of textile materials, The Textile Institute" (Manara Printing Services, London 1975).
5. J. ROBSON, J. HAGUE, G. NEWMAN, G. JERONIMIDIS and M. P. ANSELL, Survey of natural materials for use in structural composites as reinforcement and matrices, Report No. EC/431/92 to DTI LINK Structural Composites Committee, Bangor, (1993)
6. L. Y. MWAIKAMBO and M. P. ANSELL, *J. Mater. Sci.* (2003) (Submitted)
7. W. E. MORTON and J. W. S. HEARLE, in "Physical Properties of Textile Fibres" (The Textile Institute, Heinemann, London, 1975) p. 1.
8. J. GASSAN and A. K. BLEDZKI, *Comp. Sci. and Technol.* **59** (1999) 1303.
9. J. BODIG and B. A. JAYNE, in "Mechanics of Wood Composites" (Van Nostrand Reinhold Company Inc., New York, 1982) p. 335.
10. F. R. CICHOCKI and J. L. THOMASON, *Comp. Sci. Technol.* **62** (2002) 669.
11. A. G. KULKARNI, K. G. SATYANARAYANA, P. K. ROHATGI and V. KAYAN, *J. Mater. Sci.* **18** (1983) 2290.
12. P. S. MUKHERJEE and K. G. SATYANARAYANA, *J. Mater. Sci.* **19** (1984) 3925.
13. L. Y. MWAIKAMBO and M. P. ANSELL, *J. Mater. Sci. Lett.* **20** (2002) 2095.
14. A. MURKHEJEE, P. K. GANGULY and D. SUR, *J. Textile Inst.* **84** (1993) 348.
15. L. Y. MWAIKAMBO and M. P. ANSELL, *J. Appl. Polym. Sci.* **84** (2002) 2222.
16. X. LU, M. Q. ZHANG, M. Z. RONG, D. L. YUE and G. C. YANG, *Polym. and Polym. Comp.* in print
17. L. Y. MWAIKAMBO and M. P. ANSELL, *J. Mater. Sci. Lett.* **20** (2002) 2095.
18. L. Y. MWAIKAMBO, to be submitted for publication.
19. D. J. JOHNSON, in "Applied Fibre Science," Vol. 3, edited by F. Happey, (Academic Press, London 1979) p. 127.
20. A. R. SANADI, S. V. PRASAD, P. K. ROHATGI, *J. Mater. Sci. Lett.* **5** (1986) 395.
21. J. GEORGE, J. IVENS and I. VERPOEST, *I, Die Angew. Makrom. Chem.* **272** (1999) 41.
22. J. M. DINWOODIE, *Wood Sci. Technol.* **12** (1978) 271.
23. G. C. DAVIES and D. M. BRUCE, *Textile Res. J.* **68** (1998) 623.

Received 12 January
and accepted 13 July 2005